



Motion energy versus position tracking: spatial, temporal, and chromatic parameters

Qasim Zaidi^{a,*}, Jeremy S. DeBonet^b

^a *SUNY College of Optometry, 33 West 42nd St., New York, NY 10036, USA*

^b *MIT, Artificial Intelligence Laboratory, Cambridge, MA 02139, USA*

Received 27 June 1999; received in revised form 13 July 2000

Abstract

The fundamental question in motion perception is whether motion is an interpretation imposed on an object or feature perceived at separate positions at sequential instants, or whether it is the response of direction-sensitive detectors that can extract the motion-energy in the stimulus, i.e. the orientation of spatio-temporal energy. To answer this question we constructed stimuli whose position changed in one direction while the motion energy contained in the same spatial frequency moved in the same or the opposite direction (by superimposing moving sinusoidal gratings on stationary gratings of the same spatial frequency and orientation). In every case tested (0.25–25 Hz temporal frequency; 0.25–1.0 cyc/deg spatial frequency; achromatic and equiluminant contrast), the perceived direction of motion was in the direction of motion energy, indicating the existence of neurons which compute motion direction without explicitly computing spatial position. The measurements also confirmed that motion-energy computations can be modeled as separable in spatial and temporal frequency. © 2000 Elsevier Science Ltd. All rights reserved.

Keywords: Motion energy; Position tracking; Chromatic motion; Motion facilitation

1. Introduction

The motion of an object involves a change in physical position over time. The fundamental question in motion perception is whether motion is an interpretation imposed on features perceived at separate locations at different times, or whether it is the output of motion detectors analogous to those for light or contrast (Julesz, 1971; Lu and Sperling, 1995). This question can be difficult to resolve, because as Helmholtz noted, we do not perceive our sensory detectors, what we perceive is always the result of computations performed on inputs provided by sensory neurons.

A number of different types of evidence support the existence of neural computations of motion energy that are independent of any computation or representation of the spatial location of features. Exner (1875) showed that percepts of motion do not require that an object be perceived in two places at two times. Gros, Pope, and

Cohn (1996) measured luminance thresholds for motion and position discrimination, and found that for short inter-stimulus intervals, thresholds were significantly lower in the motion task. Hence comparison of perceived or remembered positions was not the basis of the perception of motion.

In the waterfall illusion, after prolonged viewing of motion in one direction, stationary stimuli appear to move in the opposite direction (Wohlgenuth, 1911). A velocity in the adapting direction can be found at which physically moving stimuli appear stationary (Sachtler & Zaidi, 1993). The remarkable aspect of the percept after adaptation is that while a stationary test stimulus appears to move, its position does not appear to change. This provides phenomenological evidence for a sense for motion that can be adapted independently of a sense for position.

Electrophysiological studies have provided direct evidence for neurons in primate visual cortex which respond more strongly to stimuli that move in one direction than to stimuli that move in the opposite direction (Hubel & Wiesel, 1959). The responses of

* Corresponding author. Fax: +1-212-7805009.

E-mail address: qz@sunyopt.edu (Q. Zaidi).

these neurons are compatible with models that extract motion energy from the outputs of contrast sensitive neurons sampling adjacent locations in visual space (Emerson, Bergen, & Adelson, 1992).

Any grey-level dynamic display can be considered a spatio-temporal luminance pattern, where luminance (L) varies as a function of spatial location and time. A stimulus moving in one spatial dimension can be succinctly depicted in a space (s) versus time (t) grey-level plot, where the velocity is given by the dominant orientation in the plot (Pearson, 1975). Pattern and motion detection both depend on the detection of frequency components. From the two-dimensional Fourier transform of the space-time plot, the magnitude of the Fourier spectrum (F) can be plotted for spatial frequency (u) versus temporal frequency (v). The effect of motion is to shear both the grey-level (s,t) representation and the spectrum in the temporal frequency domain without affecting spatial frequency, such that the orientation of energy in the frequency plot is an equivalent indicator of the speed and direction of motion to the orientation in the space-time plot (Bracewell, 1995). In fact, every pair of points in $F(u,v)$ that is symmetrically arranged around the origin represents a drifting sinusoidal component of $L(s,t)$; therefore it is possible to associate energy in particular sectors in the spatio-temporal frequency space with particular image-velocity components. By filtering specific sectors, it is therefore possible to detect image-velocity components of particular values (Adelson & Bergen, 1985; Watson & Ahumada, 1985; van Santen & Sperling, 1985). Motion-energy extracting models and direction sensitive neurons can be viewed as detecting the orientation of the Fourier energy around the (0,0) point. In this paper, we will use orientation in the modulus of the spatio-temporal frequency spectrum as our definition of the direction of 'motion-energy'.

There is, however, some evidence for feature and/or positional analysis preceding motion perception. Though an analysis in terms of oriented motion energy can explain many phenomena of the type of apparent motion described by Exner (Morgan, 1980; Watson & Ahumada, 1985), there are others that require additional processes. Braddick (1980) has provided evidence for a long-range motion mechanism that can operate over large spatial and temporal separations and may involve higher level visual information. Hochberg and Brooks (1978) used simple shapes to create a conflict between shortest path and shape identity in apparent motion, and found that at short presentations, motion was perceived across shortest paths, but at longer presentations, motion between identical shapes dominated.

When one considers motion that is defined purely by chromatic signals, the issue of position-tracking versus motion energy computation takes on additional interest. Yager and Lapierre (1975) measured spectral sensitivities for flicker-photometry and judgements of direction of

motion, and from the similarity of the curves suggested that the same achromatic system mediates both tasks. A one-dimensional, *iso*-luminant, chromatic sine-wave appears to move significantly slower than an achromatic, luminance grating of the same spatial frequency moving at the same physical speed (Cavanagh, Tyler, & Favreau, 1984). In addition, the function relating perceived speed to physical contrast is much steeper for luminance than for chromatic gratings (Hawken, Gegenfurtner, & Tang, 1994; Gegenfurtner & Hawken, 1996). In fact at low (but perceptible) contrasts, a chromatic grating moving at a slow constant velocity can appear to move in a discontinuous fashion. Since the efficiency of positional acuity for chromatic stimuli can be as high as for luminance stimuli (Krauskopf & Farrell, 1991), it is a possibility that chromatically defined motion at slow speeds is perceived through position tracking. This notion has been reinforced by the relative paucity of direction selective cortical neurons that can be driven by purely chromatic stimuli. Lennie, Krauskopf, and Sclar (1990) studied V1 cortical neurons by using the same methods used to reveal that all P-cells in primate LGN respond to chromatic contrast (Derrington, Krauskopf, & Lennie, 1984). They estimated that only a small fraction of cortical neurons responded to pure chromatic stimulation. In addition, in cortical area MT, which is composed entirely of motion sensitive neurons, Gegenfurtner, Kiper, Beusmans, Carandini, Zaidi, & Movshon (1994) found that almost every cell had a null response to chromatic modulation at a cell-specific luminance contrast that was close to the canonical CIE (1931) definition of equiluminance.

2. Methods

In this study, we present two new methods for resolving the issue of motion-energy versus position-tracking computations. To isolate motion-energy mechanisms, we used a stimulus whose position changes in a single direction, while the motion energy contained in the same spatial frequencies moves in the same or opposite direction. In a seminal study of motion perception, Lu and Sperling (1995) have exploited similar principles in their pedestal-plus-test paradigm. The similarities and differences between the two paradigms are discussed in the appropriate locations in this paper.

The basic principle underlying this method is illustrated in Fig. 1. When a sinusoidal grating of spatial frequency u_0 , moving at a constant velocity given in terms of the temporal frequency v_0 :

$$L_M = B \cos(u_0 s + v_0 t) \quad (1)$$

is added to a stationary sinusoidal grating of the same spatial frequency and orientation, but of amplitude A greater than B :

$$L_S = A \cos(u_0 s) \tag{2}$$

the combined stimulus is a sine grating whose amplitude and spatial phase oscillate in time (De Bonet & Zaidi, 1995):

$$L_C = \sqrt{A^2 + B^2 + 2AB \cos(v_0 t)} \cos \left\{ u_0 s + \tan^{-1} \left[\frac{B \sin(v_0 t)}{A + B \cos(v_0 t)} \right] \right\} \tag{3}$$

Note that the complete expression for a grating is of the form: $L_0(1 + L(s,t))$, where L_0 is the mean level. Since only the modulated components were of interest in this

study, all stimuli were presented at the same mean level, and Eqs. (1)–(3) represent only the modulated components for the sake of simplicity.

The top panel in Fig. 1a is a space versus time plot of L_M , where the grey levels correspond to the achromatic or chromatic levels of the moving grating. Time proceeds from left to right and the up and down directions in space correspond to up and down in the picture, respectively. The panel shows a grating oriented with positive slope. If one views this panel through a narrow vertical aperture, equivalent to a window in time, a sinusoidal horizontal grating is perceived through it. As the aperture is placed at progressively later instances in time, the position of the grating is seen to move successively upwards in space. It should also be noted that each successive time-sampled grating has the same frequency in the spatial dimension and the same amplitude. In such diagrams, the higher the speed of the grating, the steeper is the slope. The center panel represents the stationary pedestal L_S . The bottom panel represents the combined stimulus L_C . If one views this plot through narrow vertical apertures, one sees a sine grating of the same spatial frequency as each of the constituents, but successive apertures show that the amplitude and position both oscillate with time.

A direct method of visualizing the composition is as the vector sum of the two components in a polar space (Fig. 1b, adapted from page 303 Ronchi, 1957). As time proceeds, the head of the vector corresponding to the moving grating (L_M with amplitude B) forms circles centered at the tip of the vector corresponding to the stationary grating (L_S with amplitude A). The compound stimulus L_C is represented by the vector sum of the constituents. It is easy to visualize that the amplitude of the compound oscillates between $A - B$ and $A + B$, and that its phase oscillates between the angles formed by the two tangents to the dashed circle from the origin O .

If the compound stimulus in Eq. (3) is presented to a visual system which processes it as a unitary stimulus, and tracks the positions of features like dark or light peaks or zero-crossings, it would observe a single sine-wave, oscillating up and down, and varying cyclically in amplitude. However, the Fourier transform of the compound stimulus in spatio-temporal frequency space is the complex sum of the transforms of the two components. Since the two components have the same spatial frequency, if they are presented within the same rectangular time-space window, the spatial frequency spectrum of the compound stimulus is a pair of identical sinc functions centered, respectively on plus and minus the spatial frequency of the component gratings. The temporal frequency spectrum of the steady grating is a pair of identical sinc functions, centered at $(u_0, 0)$ and $(-u_0, 0)$. The width of the sinc function depends on the size of the presentation interval. The temporal fre-

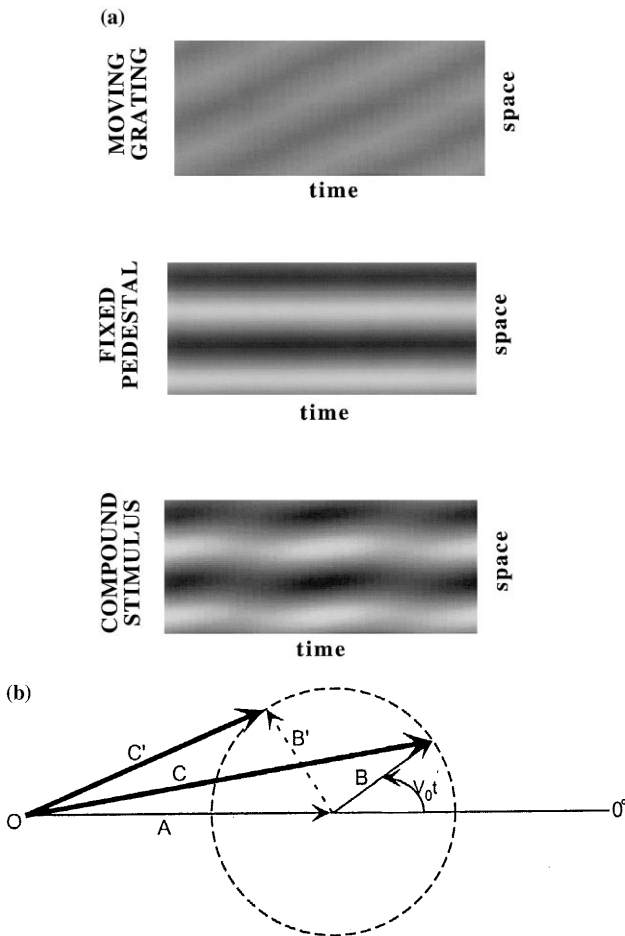


Fig. 1. (a) (Top) Space versus time plot of an upward moving horizontal sine wave grating (Eq. (1)). (Middle) Space versus time plot of a stationary vertical sine wave grating of higher amplitude than the moving grating (Eq. (2)). (Bottom) Space versus time plot of the compound stimulus formed by adding the top two stimuli. Phase and amplitude both oscillate as a function of time (Eq. (3)). (b). Depiction of the amplitude and phase of the compound stimulus as the vector sum of the stationary and moving gratings in a polar diagram. O is the origin, and 0° the polar axis. The length of a vector depicts the amplitude and the angle wrt the polar axis represents the phase of the motion. The vector A represents the stationary grating, and B and B' represent two different phases of the added moving grating, with C and C' , respectively representing the corresponding amplitude and phases of the compound stimulus. The dashed circle depicts the locus of the tip of the compound vector as time proceeds.

quency spectrum of the moving grating is sheared, so that the slope of the axis of symmetry with respect to the temporal frequency axis depends on the velocity (v_0/u_0). Thus, only the moving grating provides an oriented component to the spatio-temporal frequency spectrum. In the spatio-temporal spectrum of the compound stimulus, the magnitude and tilt of the oriented component depends on the particular presentation conditions. If for a presentation condition, an observer reliably detects the direction of motion of the moving component, irrespective of the direction of the compound motion, then that provides evidence that the oriented components of spatio-temporal energy are being discriminated reliably from the non-oriented components. This in turn provides evidence for the detection of motion by motion-energy units.

Since in general there are oriented and symmetric components to the compound spectrum, the question is how best to use this method to identify the functioning of motion-energy units. Lu and Sperling (1995) based their method on a property of Reichardt units that static displays are ignored if the stimulus is presented for one cycle plus one frame and the time-constant of the filters is longer than this interval. They further restricted themselves to a 2:1 amplitude ratio of stationary to moving grating, so as to avoid possible non-linearities before and after motion computation. We have used two quite different procedures to identify the activity of motion energy units at various spatial and temporal frequencies, for chromatic and luminance stimuli. The procedures are described in each of the experimental sections.

2.1. Equipment

All stimulus presentation and data collection were computer controlled. Stimuli were displayed on the $14.14^\circ \times 10.67^\circ$ screen of a BARCO 7651 color monitor with a refresh rate of 100 frames/s. Images were generated using a Cambridge Research Systems Video Stimulus Generator (CRS VSG2/3), running in a 90 MHz Pentium based system. Through the use of 12-bit DACs, after gamma correction, the VSG2/3 was able to generate 2861 linear levels for each gun. Any 256 combinations of levels of the three guns could be displayed during a single frame. By cycling through pre-computed look up tables we were able to update the entire display each frame.

Phosphor chromaticity specifications supplied by BARCO and gamma-corrected linearities of the guns were verified using a Spectra Research Spectra-Scan PR-650 Photospectroradiometer. Calibration and specification of colors was performed according to the methods detailed in Zaidi and Halevy (1993). Stimuli were varied along the three cardinal axes of color space (Krauskopf, Williams, & Heeley, 1982), designated as

light–dark (LD), red–green (RG) and yellow–violet (YV). In terms of relative cone excitations, the (L, M, S) coordinates of the mid-white origin W of the displayable color space were $W = (0.652, 0.348, 0.017)$, and the coordinates of the ends of the three axes were: $D = (0, 0, 0)$; $L = (1.304, 0.696, 0.034)$; $R = (0.706, 0.294, 0.017)$; $G = (0.602, 0.398, 0.017)$; $Y = (0.652, 0.348, 0.003)$; $V = (0.652, 0.348, 0.031)$. Along each axis, contrast is expressed on a scale [0.0, 1.0] where 1.0 is the maximum displayable contrast on that axis. The luminance of the screen when set to W was equal to 30 cd/m².

CRT monitors often have pixel interactions, such that vertical gratings of 2 pixels/cyc have different contrast than horizontal gratings of 2 pixels/cyc. To counter this possible artifact, in Experiment 1 we used only vertically oriented gratings, and in Experiment 2, only pairs of gratings oriented at 45° and 135° from the horizontal.

2.2. Observers

Three observers JSD, JRF and JES with normal visual acuity and color vision (ages 20–21) participated in the study. JSD, the second author, was an experienced psychophysical observer, whereas this was the first set of psychophysical measurements made by JRF and JES who were uninformed as to the purposes of the study. For all observers, the equiluminant plane was determined by flicker photometry and minimum motion techniques, and was close to the canonical CIE (1931) plane.

3. Experiment 1

3.1. Detection of motion energy orientation

3.1.1. Procedure

In the bottom panel of Fig. 1, during one half of a cycle of the periodic spatial oscillation of the compound grating, the compound grating moves in the same direction as the moving grating, but at a slower speed. During the other half of the cycle, the compound stimulus moves in the opposite direction. If the spatial phase of the stationary cosine grating is defined to be 0.0, then the ‘same-phase’ half-cycle occurs when the moving grating travels from a phase of $-\pi/2$ to $+\pi/2$, and the ‘opposite-phase’ half-cycle occurs from $+\pi/2$ to $-\pi/2$. In Experiment 1, each test interval consisted of one or the other of these half-cycles.

Four types of test intervals were used, each consisting of one of the two types of half-cycles and one of two pedestal conditions, ‘flashed’ and ‘steady’. In the ‘flashed’ pedestal condition, the stationary grating was flashed on and off with the half-cycle of motion, and

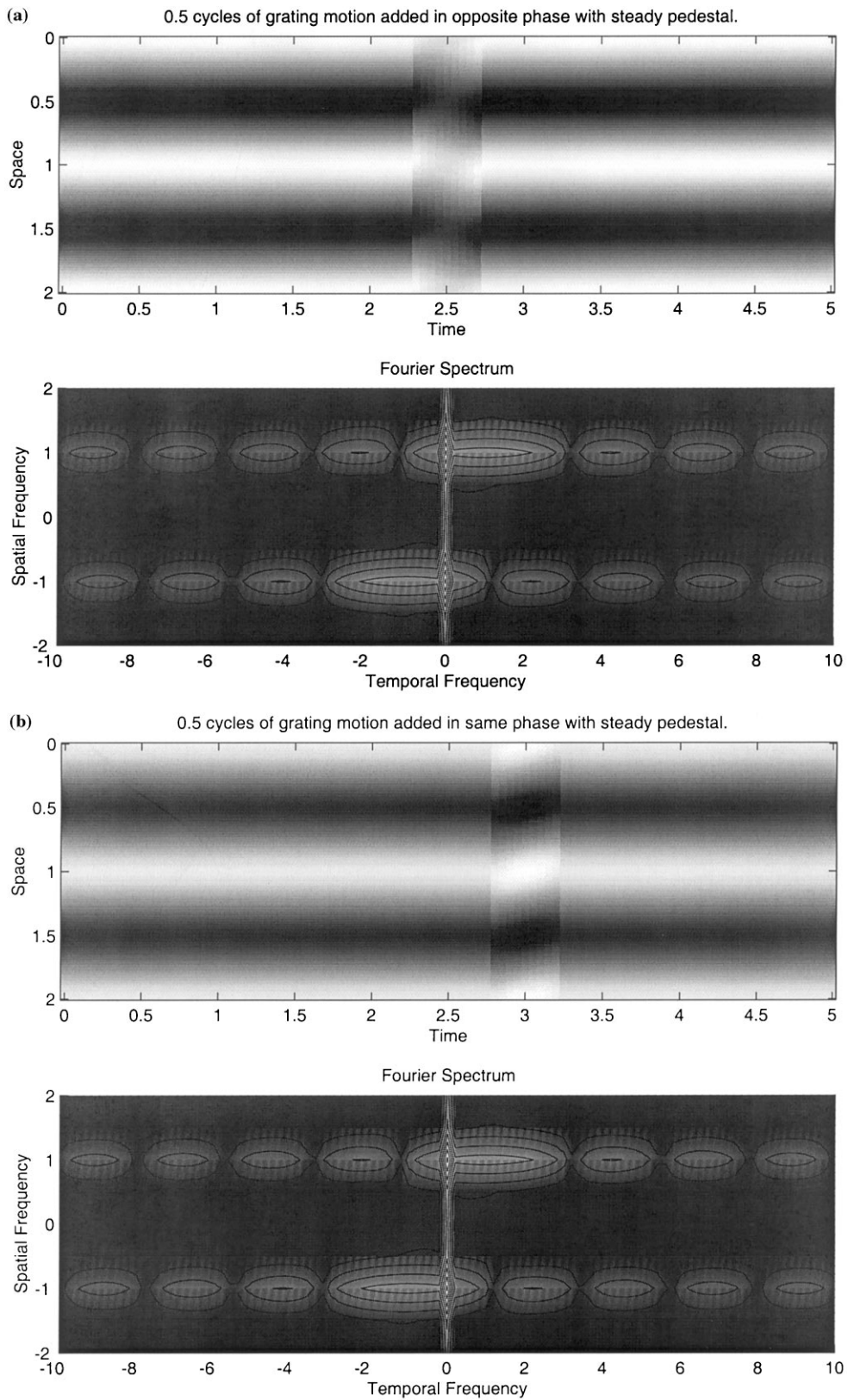


Fig. 2. (Continued)

the inter-test interval consisted of a uniform grey screen at mean luminance. In the ‘steady’ pedestal condition, the stationary grating was presented continuously during

the half-cycles of motion and the inter-test interval.

The rationale for these four test conditions will be explained using the illustrations in Fig. 2 for moving

horizontal gratings of 1.0 cpd (cyc/deg) drifting upwards at 1.0 Hz, superimposed on stationary gratings of the same spatial frequency and orientation. The contrast

ratio of the pedestal to the moving grating is 4:1.

The critical condition shown in panel (a), consists of the moving grating drifting upwards added in the oppo-

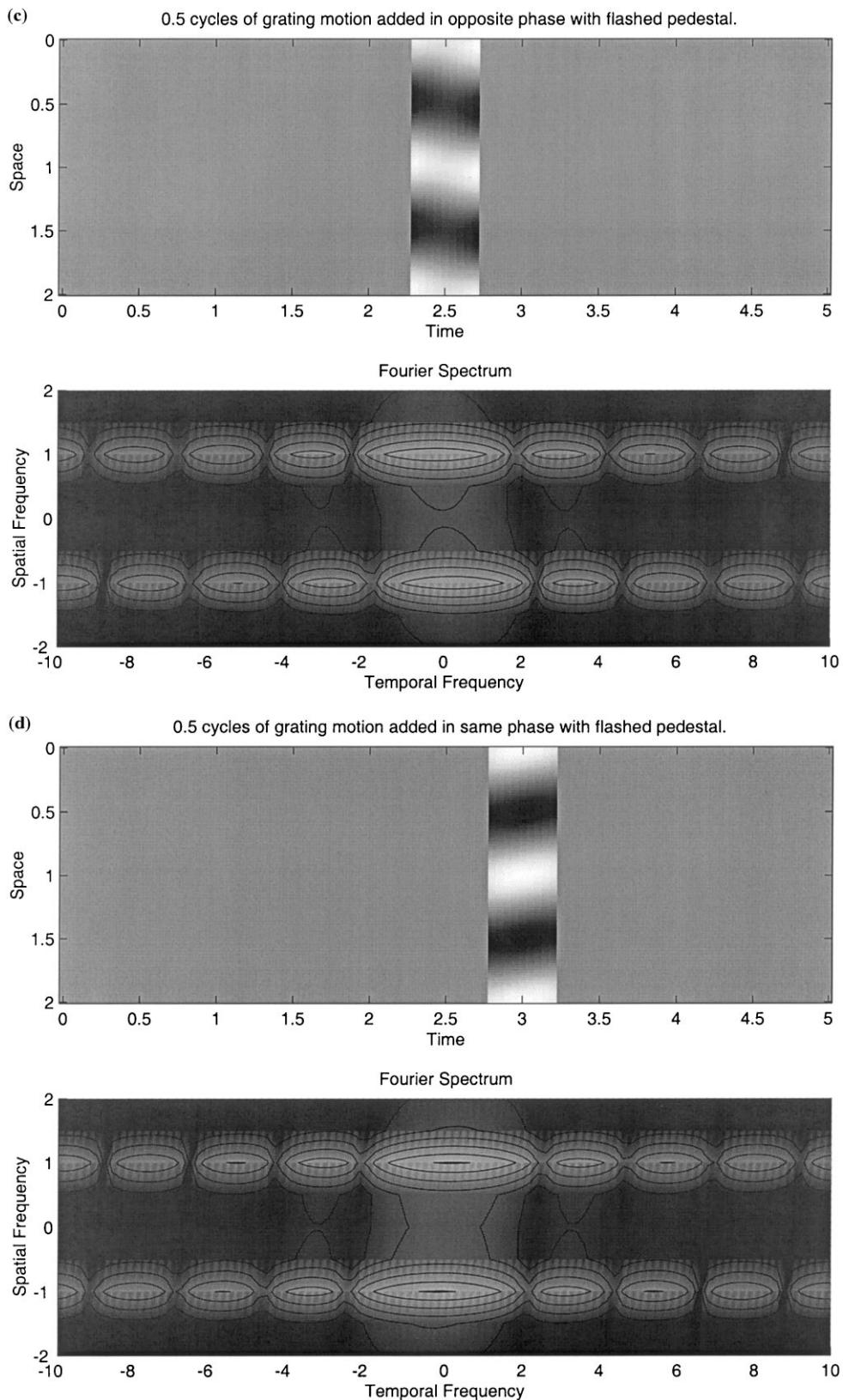


Fig. 2. (Continued)

site-phase half-cycle to the steady stationary pedestal. The top picture in the panel is a space–time plot of one trial of this condition. Till the 2.25 second point, only the steady pedestal is presented, then the moving grating is added for a half-cycle. Notice that because this is the opposite-phase cycle, the compound stimulus moves down even though the moving grating moves upwards.

The picture directly below shows the Fourier spectrum of this trial. In the grey-level picture, the lightness is a monotonic function of the modulus of the Fourier transform [$\log(|F(u,v)| + 0.001)$]. Since the gratings are sinusoids of 1.0 cpd, the energy is concentrated around the $+1$ and -1 co-ordinates on the vertical axis. The smearing of spatial frequency is caused by the limited window presented on the screen. The $(0,0)$ point represents the transform of the mean level and provides a convenient reference point (There should be a bright spot at this point representing the mean luminance, but for the sake of dynamic range in the picture it has been removed). The bright vertical bands at zero temporal frequency constitute the spectrum of the stationary pedestal. To simplify mathematical expressions of the Fourier spectra, it helps to assume that the spatial extent of the stimulus is very large. Then for the steady pedestal ($-A \cos(u_0, s)$), the Fourier transform is:

$$2A\pi^2[\delta(u + u_0) + \delta(u - u_0)]\delta(v) \quad (4)$$

i.e. the spectrum is real with power at $(u_0, 0)$ and $(-u_0, 0)$. The temporal frequency spectrum of the moving grating is broader due to the short presentation interval, and is sheared due to upward motion, so that the axis of symmetry has a positive slope. The Fourier transform of the pulsed moving grating is:

$$B \frac{\pi^2}{v_0} \left[\delta(u + u_0) \text{sinc} \left(\frac{(v + v_0)\pi}{2v_0} \right) + \delta(u - u_0) \text{sinc} \left(\frac{(v - v_0)\pi}{2v_0} \right) \right] \quad (5)$$

At $u = u_0$ the transform is a sinc function centered at $v = v_0$ with the width of the center lobe being $4v_0$, and at $u = -u_0$, a similar sinc function centered at $v = -v_0$. The spectrum of the compound stimulus is just the sum of the two constituent transforms, and as shown in Fig. 2a, in the modulus of the transform the oriented

component contributed by the moving grating is not altered by the spectral contribution of the steady pedestal. Therefore, despite the downward motion of the compound stimulus during the test interval, the orientation of energy in the spectrum of the stimulus remain indicative of upward motion. Consequently, a visual system will detect downward motion if its computations are based on the changes in position of the compound stimulus, and will signal upward motion if its computations extract the orientation of Fourier energy.

Fig. 2b–d provide control conditions for the experiment. In Fig. 2b, the moving grating is added for a half-cycle to the steady grating in the same-phase condition. The space–time plots in Fig. 2a and b illustrate that the direction of motion of the compound stimulus in the test interval has changed from downwards in (a) to upwards in (b). So a system which tracks the compound stimulus would perceive opposite directions of motion for the conditions depicted in (a) and (b). The Fourier spectra in (a) and (b), however, indicate identical upwards motion [Note: A mathematically equivalent way of describing the same-phase wrt the opposite-phase condition is to keep the phases of the two components fixed but to negate the amplitude of the stationary pedestal. This has the effect of negating the Fourier spectrum in Eq. (4). In the steady pedestal case, the spectrum of the compound is negligibly changed, but see below for changes in the flashed pedestal case]. Notice that the amplitude spectra of the two stimuli have identical spatial-temporal frequency contents. An observer basing decisions on the detection of oriented Fourier energy would perceive motion in the same directions in conditions (a) and (b). A comparison between perceived directions of motion in the conditions depicted by these panels is thus a critical test between position based and energy based computations of motion.

In Fig. 2c and d, the moving and stationary gratings are both flashed simultaneously for a half-cycle of movement. In (c) the moving grating is added in the same opposite-phase interval as in (a). The space–time plots show that inside the test interval, identical stimuli are presented in the conditions depicted in (a) and (c). However, the orientation of the Fourier spectrum in (c)

Fig. 2. (a–d). All four sections show a pair of grey-level pictures depicting the four conditions in Experiment 1. The top picture consists of a space time plot of the stimulus, half a temporal cycle of a moving horizontal 1.0 cpd grating drifting upwards at 1.0 Hz superimposed on a stationary grating of the same spatial frequency. The conditions differ in the relative phases of the two gratings and whether the stationary grating was ‘steady’ throughout the experiment, or just ‘flashed’ in concert with the moving grating. The slope of the grating inside the test interval gives the direction of motion of the compound stimulus. The bottom picture shows the log of the modulus of the Fourier spectrum of the top picture, i.e. spatial frequency versus temporal frequency. The dominant orientation of the spectrum wrt the $(0,0)$ point gives the direction of motion energy in the stimulus. (a) Moving grating added in opposite phase to steady pedestal. The compound stimulus moves down, but the orientation of the Fourier spectrum indicates upward motion energy. (2) Moving grating added in the same phase as the steady pedestal. Both the compound stimulus and the Fourier spectrum indicate upward motion. (c) Moving grating added in opposite-phase to flashed pedestal. Both the compound stimulus and the Fourier spectrum indicate downwards motion. (d) Moving grating added in the same phase as flashed pedestal. Both the compound stimulus and the Fourier spectrum indicate upwards motion.

is orthogonal to that in (a). Thus another test of position versus energy based motion computations is that position-tracking predicts motion percepts in the same direction in these two conditions, whereas motion-energy predicts percepts in opposite directions. In Fig. 2d the moving grating was added in the same-phase condition as in (b), i.e. identical stimuli were presented inside the test interval in the two conditions. In addition, the orientation of motion energy is similar in (b) and (d). Unlike in (a) and (b), the temporal frequency spectra of the stationary gratings in (c) and (d) are broad enough to substantially overlap with the spectra of the moving gratings. Since the compound spectrum is the sum of the constituent spectra, the orientation of the compound spectrum is affected by the relative phase of the stationary and moving gratings.

The Fourier transform of the stationary pedestal pulsed for the half-cycle

$$\left[\frac{-\pi}{2v_0}, \frac{\pi}{2v_0} \right] \text{ is } A \frac{\pi^2}{v_0} \text{sinc}\left(\frac{v\pi}{2v_0}\right) [\delta(u - u_0) + \delta(u + u_0)] \quad (6)$$

i.e. real sinc functions of v centered at $(-u_0, 0)$ and $(u_0, 0)$. Again the opposite phase pedestal can be assumed to have an amplitude of $-A$. These sinc functions have the same width as the sinc functions contributed by the moving grating (Eq. (5)), and hence overlap considerably. The compound spectrum is sheared with positive or negative slope, based on the relative signs of the component spectra. The moduli plotted in Fig. 2 are all positive.

The four conditions together provide critical tests of position-tracking versus motion-energy computation at every fixed combination of spatial and temporal frequency for gratings along any color axis. If the observer is extracting motion energy, then motion illustrated in Fig. 2a,b and d should be seen in the direction of the moving grating, whereas motion illustrated in Fig. 2c (flashed plus opposite-phase) should be seen in the opposite direction. On the other hand, if the observer is tracking positions of the compound grating, then in (b) and (d), the in-phase conditions, motion should be seen in the same direction as the moving grating, whereas in (a) and (c), the out-of-phase conditions, it should be seen in the opposite direction.

3.2. Stimulus parameters

Measurements were made inside a centrally fixated 12° disk, at temporal frequencies of 0.25, 1.0, 16.7 and 25 Hz, and at spatial frequencies of 1.0 and 0.25 cyc/deg and with achromatic light–dark and equiluminant red–green and yellow–violet vertical gratings.

To equate the effectiveness of the pedestals for the different spatial frequencies, presentation lengths, and color directions, the pedestals were set to 0.0, 4.0 and 8.0 times the detection threshold for a stationary grating, measured separately for each condition.

Psychometric curves for the detection of motion as a function of the contrast of the moving grating were measured for each condition using a method of constant stimuli (ten trials per point). All conditions for each pedestal were randomly interleaved. On each trial the observer pressed buttons to indicate whether the perceived direction of motion was leftwards or rightwards. For all three color axes, contrast was measured on a scale of 0 to 1.0 where 1.0 was the maximum displayable contrast.

A small fixation dot in the center of the display was visible throughout the experiment.

3.2.1. Results

Results for observers JSD, JRF and JES are shown in Figs. 3 and 4, respectively. Psychometric curves for the probability of perceiving motion in the direction of the moving grating are plotted versus the contrast of the moving grating times 1000. Going down the figures, results are presented for (i) LD gratings at 0.25 cyc/deg (25.0 Hz, 16.7 Hz, 1.0 Hz), (ii) LD at 1.0 cyc/deg (16.7 Hz, 1.0 Hz), (iii) RG at 0.25 cyc/deg (16.7 Hz, 1.0 Hz), (iv) YV at 0.25 cyc/deg (16.7 Hz, 1.0 Hz). The results, presented in columns from left to right, are for pedestals at (i) zero amplitude, (iia) steady at four times threshold, (iib) flashed at four times threshold, (iia) steady at eight times threshold, (iiib) flashed at eight times threshold. The steady pedestal and flashed pedestal conditions are depicted by circles and squares, respectively, and the same and opposite phase additions by filled and open symbols, respectively.

The most significant result is that, in every case, the perceived direction was in the direction of the motion energy even when the compound stimulus was moving in the opposite direction. For each color direction, spatial frequency, and temporal frequency, when the four curves for each pedestal amplitude are compared, the perceived directions of motion are reliably predicted by motion energy extraction. Motion in both steady pedestal conditions and in the same-phase flashed pedestal condition is seen in the direction of the moving grating. Motion is seen in the opposite direction only for the opposite-phase flashed pedestal condition. We thus find evidence for motion energy extraction at all temporal frequencies tested, for luminance (1.0–25.0 Hz), and for equiluminant red–green, and yellow–violet stimuli (1.0–16.7 Hz).

A second significant result predicted by motion energy extraction is that the amplitude of the steady pedestal should not affect sensitivity to the direction of the moving grating. This prediction follows because the

oriented energy in the spectrum of the compound stimuli is essentially not affected by the spectrum of the steady pedestal (Fig. 2). This prediction is validated in two ways by the data. First, in the steady pedestal conditions (Figs. 3 and 4), the same-phase psychometric curves are essentially the same as the opposite-phase curves, despite greater contrast of the compound stimulus in the same-phase condition. Second, this prediction is further validated by considering threshold contrast of the moving grating needed for motion energy extraction. Contrast thresholds were estimated from the 80%

point of the best fitting Weibull curve in the steady pedestal condition. In Fig. 5, the log of this contrast is plotted versus the amplitude of the pedestal (in threshold units). For both 1.0 and 16.7 Hz motion, thresholds are essentially the same for pedestal amplitudes at eight times threshold as at four times, thus matching this prediction.

An interesting facet of Fig. 5 is that the presence of a steady pedestal significantly reduces the contrast required to reliably extract the direction of motion energy for gratings moving at 16.7 Hz for both spatial frequen-

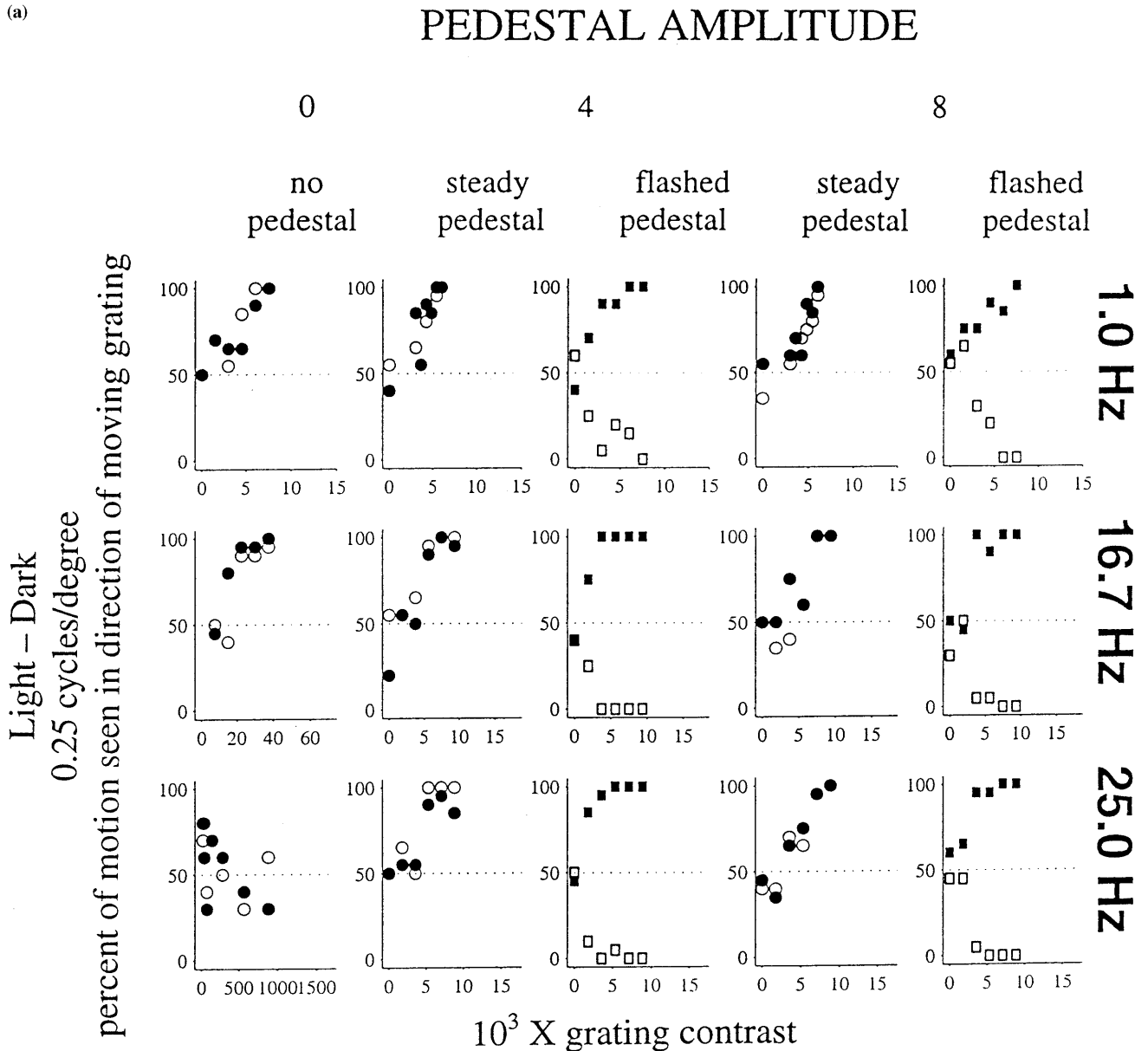


Fig. 3. Results of Experiment 1 for observer JSD. The probability of perceiving motion in the direction of the moving grating is plotted versus the contrast of the moving grating times 1000, for each of the four conditions. Symbols: Grating added in same phase as the steady pedestal (\bullet). Grating added in opposite phase to the steady pedestal (\circ). Grating added in same phase as the flashed pedestal (\blacksquare). Grating added in opposite phase to flashed pedestal (\square). For the no-pedestal condition, the open and closed symbols separately depict leftward and rightward motion. The temporal frequency of the moving gratings, the amplitudes of the pedestals in threshold units, and the common color axes of the two constituent gratings are indicated along the panels.

(d)

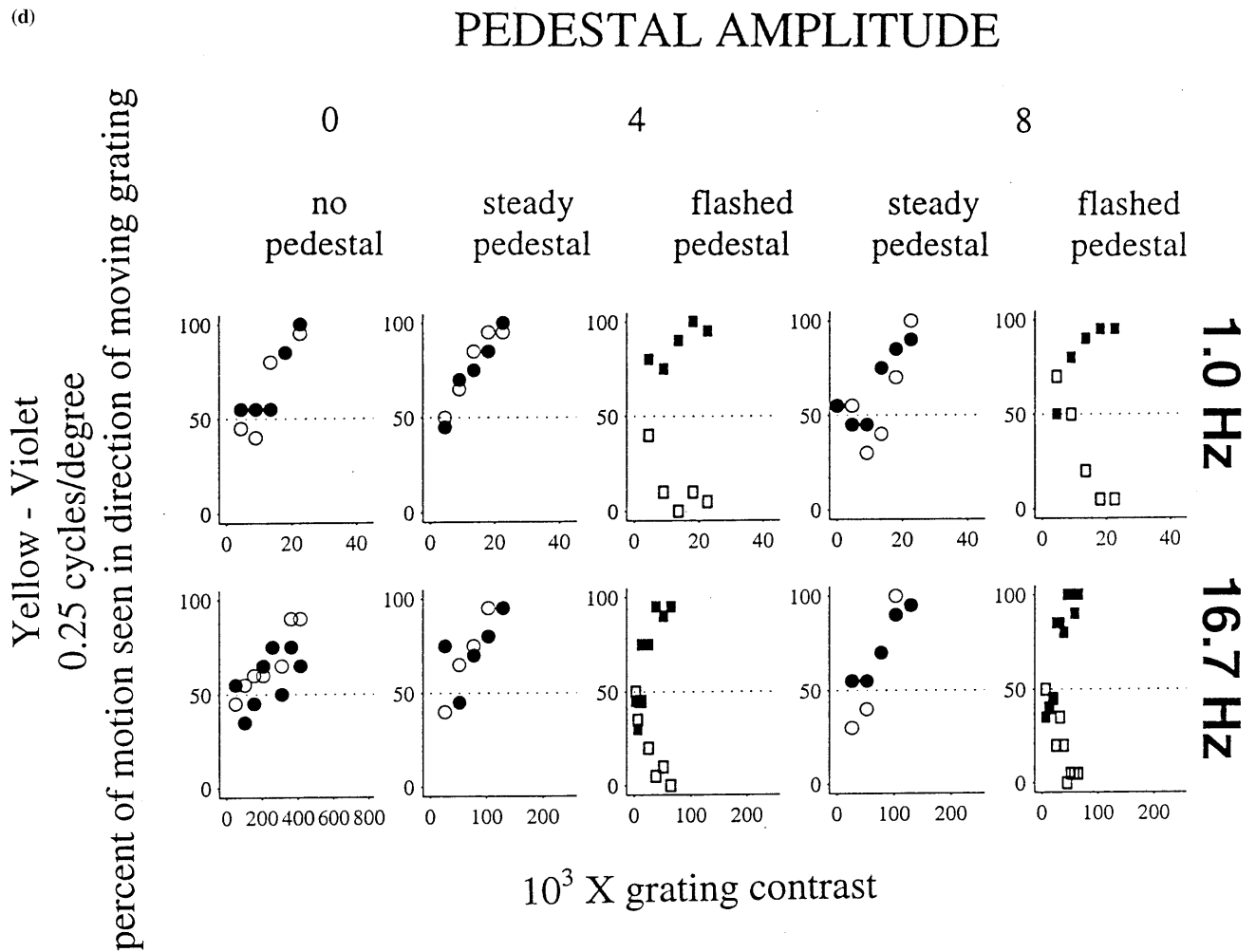


Fig. 3. (Continued)

In each panel 1000 times the contrast at threshold of the moving grating is plotted versus the number of temporal cycles in the test interval. Thresholds for detecting the motion axis are represented by circles and thresholds for detecting the motion direction by crosses.

The most salient feature of the data is that for all the two-cycle presentation conditions, thresholds for detecting motion direction were essentially equal to thresholds for detecting the motion axis, confirming the hypothesis that motion-energy was extracted at motion threshold. These results provide evidence for the existence of motion mechanisms, sensitive to luminance and chromatic energy, that function at temporal frequencies from 1.0 to 16.0 Hz.

There is, however, a significant difference between the luminance and chromatic results for the 1 cycle presentation conditions. In the luminance conditions, thresholds for motion axis are substantially lower than thresholds for motion direction, whereas for the two chromatic axes, the sets of thresholds are virtually identical. The causes of this difference are not entirely

clear to us. The Fourier transform for an n -cycle presentation of the moving grating is:

$$B \frac{2n\pi^2}{v_0} \left[\delta(u + u_0) \text{sinc}\left(\frac{n\pi(v + v_0)}{v_0}\right) + \delta(u - u_0) \text{sinc}\left(\frac{n\pi(v - v_0)}{v_0}\right) \right] \quad (7)$$

The transform for an n -cycle presentation of the stationary stimulus in cosine phase is:

$$A \frac{2n\pi^2}{v_0} \text{sinc}\left(\frac{n\pi v}{v_0}\right) [\delta(u - u_0) + \delta(u + u_0)] \quad (8)$$

As in the half-cycle presentations, the sinc functions are centered at (u_0, v_0) and $(-u_0, -v_0)$ for the moving grating and $(u_0, 0)$ and $(-u_0, 0)$ for the pedestal. The widths of the central lobes of the sinc functions decrease proportional to the number of cycles in the presentation, thus decreasing the overlap between the stationary and moving spectra. Fig. 9 shows the transforms of each of the components versus the temporal frequency for 1 cycle (top) and 2 cycle (bottom) presen-

tations for 1 Hz motion, and $A = 0.4$, $B = 0.1$. Each panel depicts the positive (u, v) quadrant at the center of the positive component of the shared spatial frequency of the components. It is clear that the oriented components of the spectrum contributed by the moving grating are less affected by the spectrum of the pedestal in the 2-cycle condition. For observer JSD, we compared the spectra of the two conditions at one cycle presentations at threshold. Though both 1 cycle spectra contained components that were symmetric around the (0,0) point, the spectrum at motion direction threshold was considerably more asymmetric. In fact, the spectra at motion direction threshold for the 1 and 2 cycle presentations were very similar, indicating that a similar amount of asymmetry in the spectra was required for the detection of motion direction.

In Fig. 10, we have plotted the sensitivity to motion energy (1/direction threshold) for the different 2 cycle presentations. The results are plotted on a log-log scale. The sets of points for the two LD spatial frequencies (0.25 and 1.0 cyc/deg) form curves that are almost parallel to each other, suggesting that motion-energy

computations could be modeled as separable in spatial and temporal frequency.

5. Experiment 3

5.1. Controls for chromatic motion-energy detection

Since chromatic mechanisms are generally considered to be slower than achromatic mechanisms, we wanted to ascertain that at high temporal frequencies like 16.0 Hz the moving chromatic stimuli were being detected by chromatic motion-energy mechanisms, as opposed to luminance driven mechanisms. For this purpose we performed two sets of ancillary measurements on observer JSD.

5.1.1. Procedure

First, we wanted to exploit the finding from Experiment 1 that at 16.7 Hz the presence of a pedestal reduced threshold for detecting the direction of the moving grating, to test whether a pedestal at an orthog-

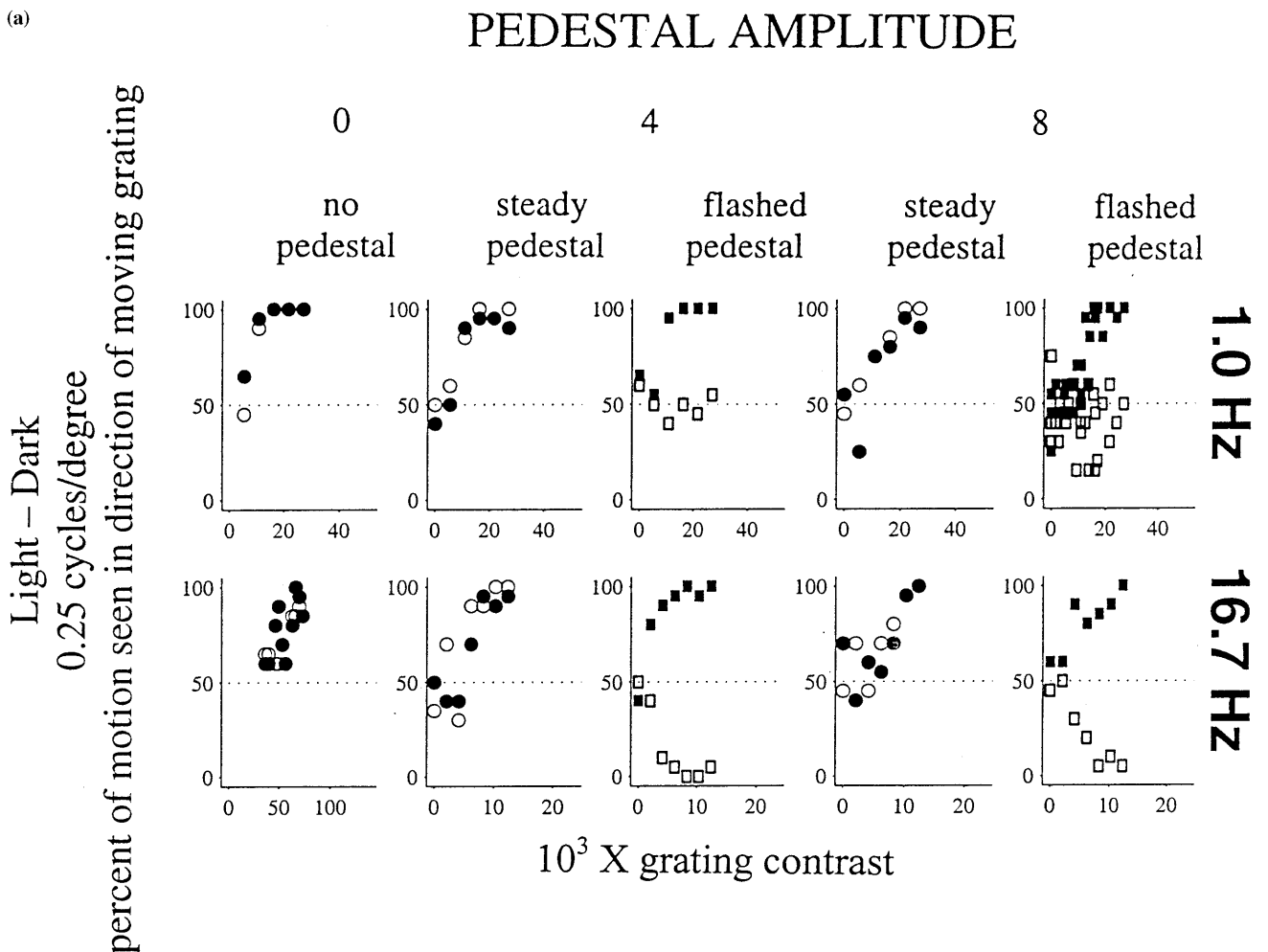


Fig. 4. Results of Experiment 1 for Observers JES (LD) and JRF (RG and YV) plotted like Fig. 3.

(b)

PEDESTAL AMPLITUDE

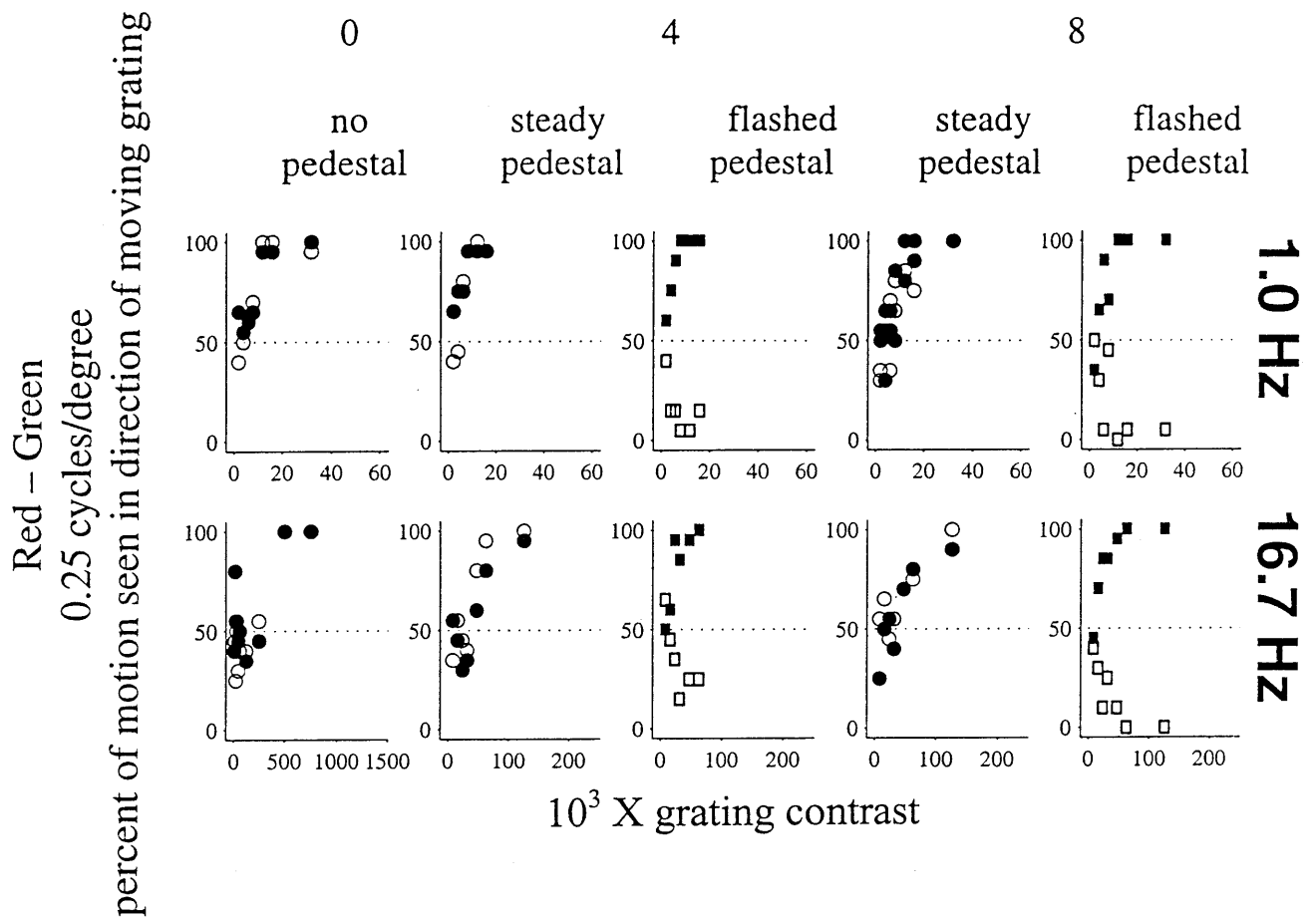


Fig. 4. (Continued)

onal color axis would evoke a similar enhancement. We repeated Experiment 2 at 16.0 Hz, but with plaid pedestals of either the same or of an orthogonal color axis, at 0.0 and 4.0 times threshold.

Second, to compare the sensitivities of directional to non-directional mechanisms, we did a variant of Experiment 2 with no pedestal. In one set of trials, a grating was counterphase modulated at 16.0 Hz and presented along one of the diagonal axes, and the observers' 2AFC task was to identify the axis. In the second set of trials a moving grating was presented in the absence of a pedestal and as in Experiment 2 the observer had to identify the direction of motion. The presentation interval in both procedures was 500 ms.

5.1.2. Results

The results of the first procedure are shown in Fig. 11. Thresholds for detecting the motion direction of the moving grating are plotted versus the color axis of the plaid pedestal. Each panel shows thresholds on zero pedestals, on pedestals of the same color axis and on pedestals of an orthogonal color axis.

In all three panels, the presence of a pedestal of the same color as the moving grating facilitated motion detection by a factor slightly greater than three times, whereas the presence of a pedestal of an orthogonal color axis did not facilitate motion detection. These results have a number of implications. First, the presence of a stationary pedestal per se did not necessarily facilitate motion detection, i.e. the pedestal did not act like a facilitating stationary landmark. Second, the facilitation effect occurred within independent color mechanisms, suggesting inhibition between temporal mechanisms tuned to the same color axis. Third, since the RG plaid facilitated detection of RG motion but not of LD motion, it is unlikely that the 16.0 Hz motion of the RG grating was being detected by an achromatic mechanism (see Cropper & Derrington, 1996 for no effect of LD pedestals on moving RG gratings).

The results for the second procedure are shown in Fig. 12. From left to right, for each of the color axes, thresholds for detection of motion direction at 16.0 Hz

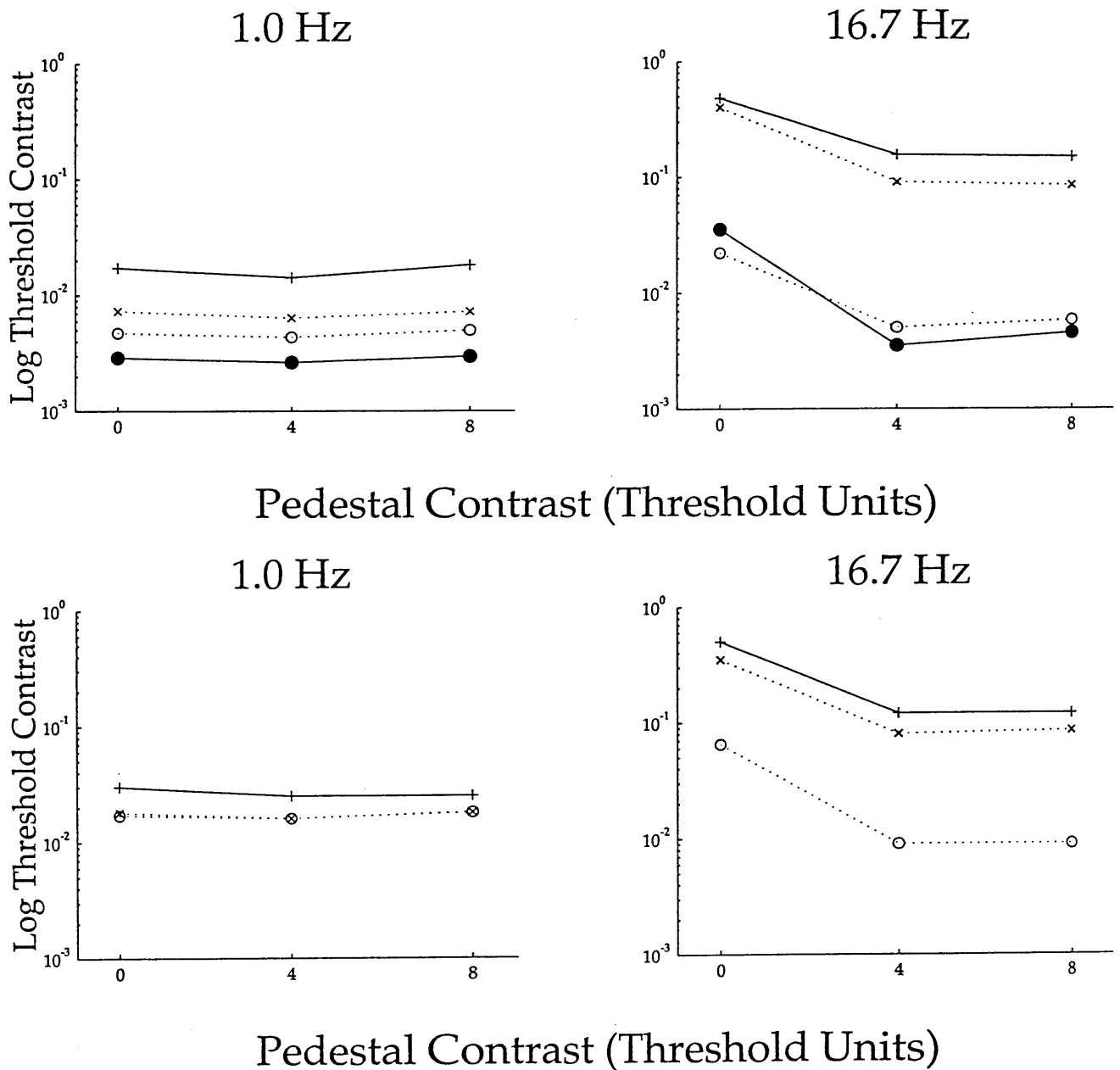


Fig. 5. The log of the threshold contrast of the moving grating in the steady pedestal condition is plotted versus the amplitude of the pedestal in threshold units, separately for 1.0 and 16.7 Hz motion. Symbols: LD 0.25 cyc/deg (o), LD 1.0 cyc/deg (●), RG (x), YV (+). Top panel JSD, bottom, JES and JRF.

ods, have revealed chromatic direction selective neurons in area V3 (Gegenfurtner, Kiper, and Levitt, 1997). It is probable that the motion-energy mechanisms revealed in this paper correspond to these neurons. It is well established that area V1 includes direction selective neurons responsive to luminance, but not to pure chromatic motion. Kiper, Fenstemaker, and Gegenfurtner (1997) also report the lack of chromatic direction selective neurons in V2. The psychophysical and perceptual differences between luminance and chromatic motion may well be due to the later formation of direction selective chromatic neurons. It is worth pointing out

that there are other important image motion properties, like motion boundaries, that are not extracted by the MT stream (Sachtler and Zaidi, 1995; Reppas, Niyogi, Dale, Sereno, & Tootell, 1997).

The issue of position tracking versus motion energy is fundamental and has been attacked by a number of psychophysical methods including Kulikowski and Toulhurst (1973), Morgan (1979, 1980), Thompson (1982), Cavanagh (1992), Lu and Sperling (1995), Cropper and Derrington (1996). The methods used in this paper are closest to the methods used in the seminal study of types of motion by Lu and Sperling (1995).

There are however a few differences. Lu and Sperling used moving grating to pedestal contrast ratios of 1:1 and 1:2. At these ratios, there is substantial asymmetry in the phase oscillations of the compound stimulus, and a practised observer could learn to use the asymmetry to guess the direction of the moving grating. In addition, as is obvious in Fig. 1, the contrast of the compound stimulus is higher when it is moving in the direction of the moving grating, than when it is moving in the opposite direction. At a contrast ratio of pedestal to moving grating of 2:1, this difference is very noticeable and could be used as a cue to motion direction by a well-practised observer. Further, when neural signals arrive at the cortical site of motion computation, a physical contrast ratio of 2:1 between the stationary and moving components may have been converted to a smaller ratio by band-pass pre-cortical processing for luminance, and to a much larger ratio by low-pass pre-cortical processing for equiluminant stimuli. We aimed to equate the effective ratio across color axes by setting pedestals in equal threshold units, and measuring the threshold contrast of motion signals. As shown in Fig. 9, depending on the relative amplitudes, a 1 cycle presentation may not contain enough asymmetry in the compound Fourier spectrum to excite motion-energy mechanisms.

Like all methods, the methods in this paper have limitations. The half-cycle method provides a series of critical controls, but requires the observer to ignore the transient changes at the onsets and offsets of the test intervals in the steady pedestal conditions. This took a little practice, but the fact that observers reported identical directions of motion in the same-phase and opposite-phase conditions showed that they were able to discount the transients which were in opposite directions in the two conditions. The plaid pedestal tasks in Experiments 2 and 3 were advantageous in being ex-

remely comfortable for observers, but were disadvantageous in running at half the frame-rate due to interlacing the two components of the plaid, and required that the moving grating contrast be a small fraction of the contrast of the pedestal. In addition, it was considerably easier to maintain fixation during the shorter presentations in Experiment 1. Taken together, these two procedures provide objective methods for distinguishing between position-tracking and motion-energy extraction for any combination of single spatial and temporal frequencies.

Classes of stimuli in which observers reliably perceive motion are second-order patterns consisting of drifting texture contrast (Chubb & Sperling, 1988), spatial contrast modulation (Johnston & Clifford, 1995), texture type (Ramachandran, Rao, & Vidyasagar, 1973), or other spatial variations that are transparent to the presumably linear spatial filtering done by motion-energy units. However, motion perception of these patterns can be explained in terms of spatially non-linear pre-processing that makes the spatial variations in the pattern visible to a later stage of motion-energy extraction (e.g. Chubb & Sperling, 1989) and does not require explicit computation of position or features (Lu & Sperling, 1995).

In addition, there is evidence that local motion percepts can be altered by the presence of multiple motion stimuli in the visual field. The most famous is the aperture effect, where the perceived direction of a moving stimulus can be altered by the shape of the stationary window through which the stimulus is viewed (Wuerger, Shapley, & Rubin, 1996). Additionally, two one-dimensional motion stimuli can be seen to cohere or move independently, in the direction of the energy-less beat, depending on non-motion properties of the stimuli (Wuerger et al., 1996; Adelson & Movshon, 1982). Finally, the spatial profile of the velocity field

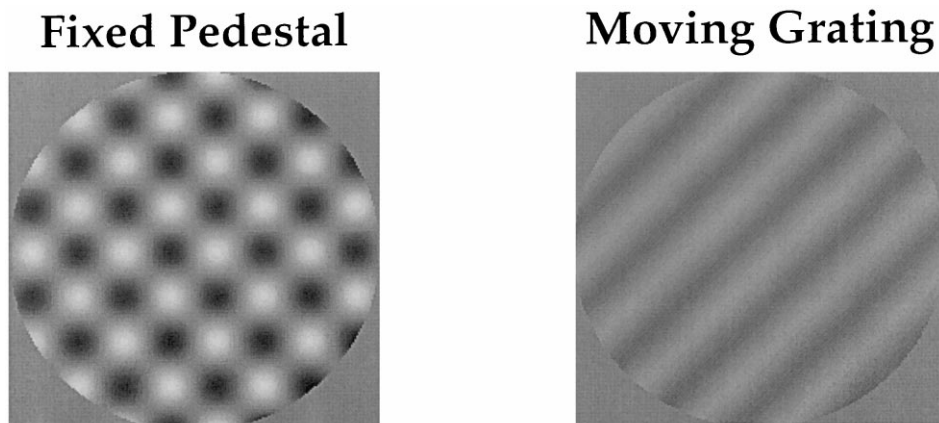


Fig. 6. Depiction of stimuli for Experiment 2. The pedestal consisted of a stationary plaid with gratings of the same spatial frequency and amplitude oriented at 45° and 135°. The moving grating was oriented at 45° or 135°, and had the same spatial frequency as the pedestal grating.

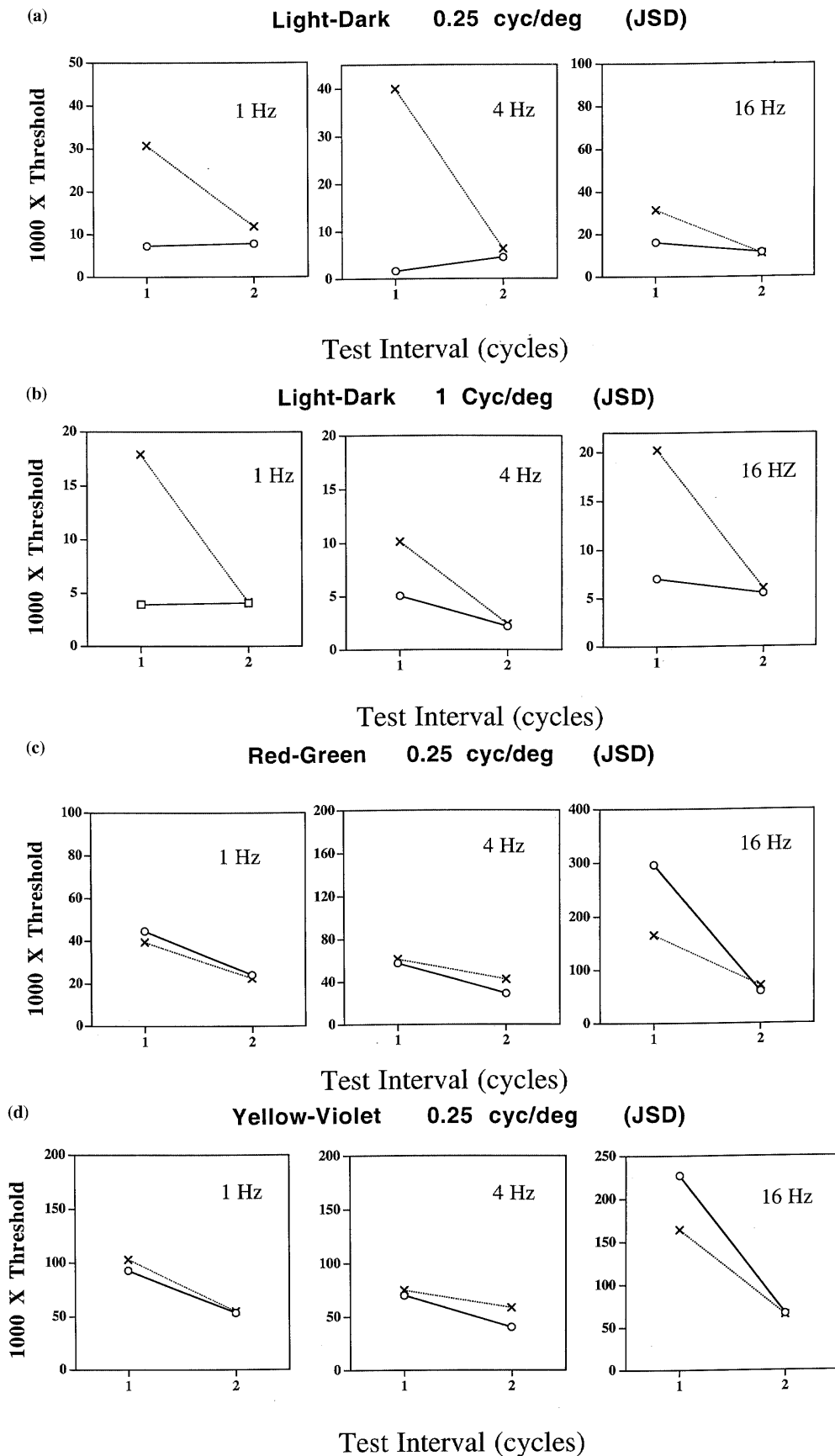


Fig. 7. Results for JSD for Experiment 2. Threshold contrast of the moving grating times 1000 is plotted versus the number of temporal cycles in the test interval. Open circles represent motion-axis thresholds, and crosses represent motion direction thresholds.

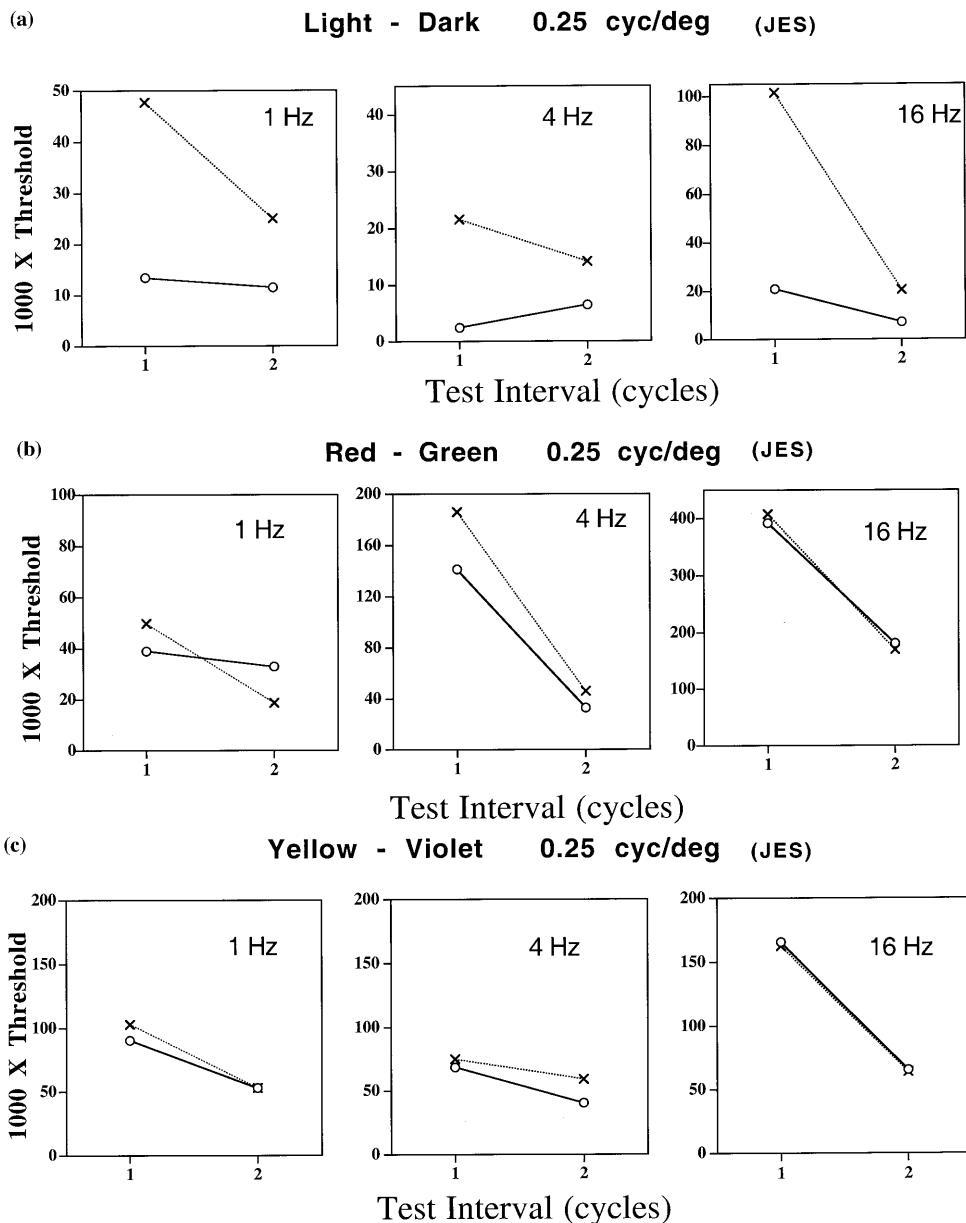


Fig. 8. Results for JES for Experiment 2, plotted similar to Fig. 7.

can influence the detection of motion. In particular, the visual system is extremely sensitive to sharp motion boundaries in the central visual field (Sachtler & Zaidi, 1995). These effects, however, have all been explained in terms of operations on the outputs of elementary motion-energy neurons.

Since Fig. 5 was presented at ARVO 1995 and ECVF 1995, other authors using different methods have also reported the facilitating property of stationary pedestals in the direction of motion (Cropper & Derrington, 1996; Zeman, Stromeyer, Chaparro, & Kronauer, 1998). The results of Experiments 1 and 3 clear up some aspects of the facilitation effect, but others remain puzzling. The first clear point is that the facilitation is not due to the pedestal acting as a perceived extended

stationary landmark against which motion can be detected, because pedestals of orthogonal color axes are if anything more salient as landmarks than pedestals of the same color axes, and yet do not facilitate detection. Second, the facilitation is similar for each temporal frequency irrespective of spatial frequency and color axis. In particular, there was a 4-fold difference in spatial frequency between the two types of LD stimuli in Experiment 1, yet the facilitation was similar. Consequently, the facilitation effect is probably based on the relative temporal frequency contents of the pedestal and moving grating, rather than velocity.

A few puzzles remain for further investigation. First, the facilitation in Experiment 1 is similar for steady and flashed pedestals, even though they make quite different

contributions to the compound spatio-temporal frequency spectrum (Fig. 2). It is clear though, that since the steady pedestal facilitates motion-energy detection without significantly affecting the energy of the oriented Fourier components (Fig. 2a), therefore the facilitation is unlikely to be due to the explanation provided by Zeman et al. (1998) that the effect is due to the visual system's higher sensitivity to the difference of the contrast of right versus left moving components than to either component alone. Second, the facilitation is con-

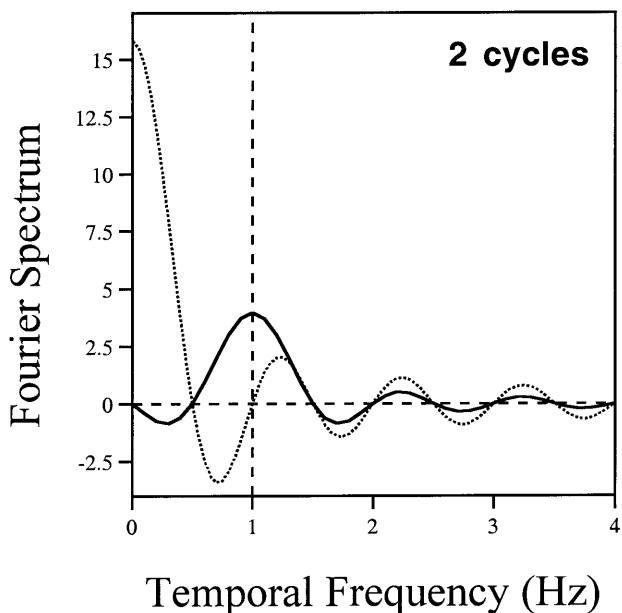
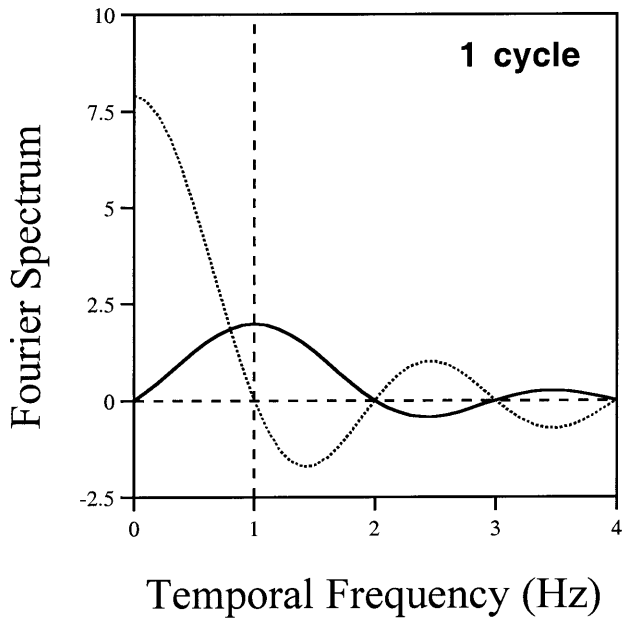


Fig. 9. Fourier spectra of the moving (solid line) and stationary (dashed line) gratings for 1 cycle (top) and 2 cycle (bottom) presentations. Just the positive (u, v) quadrant is shown.

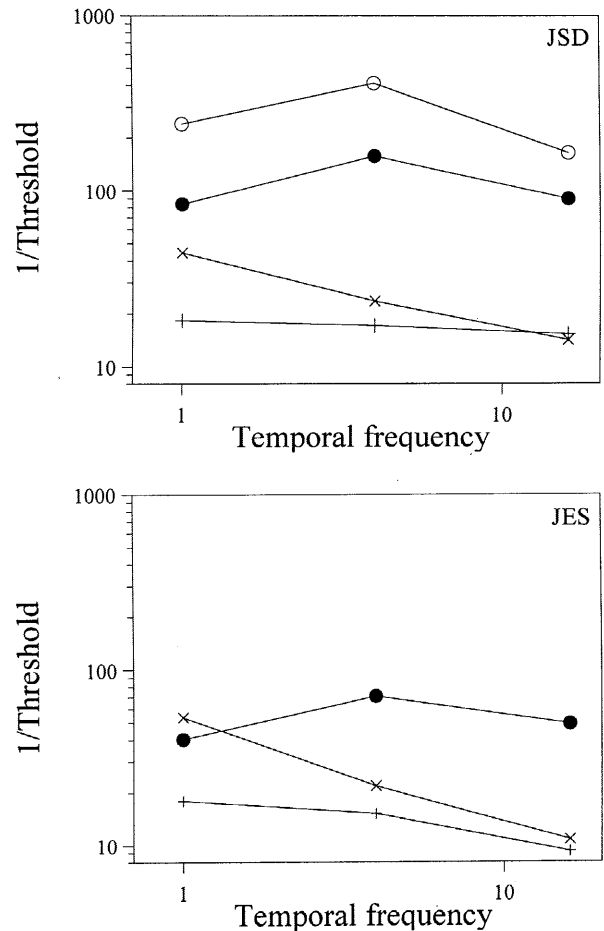


Fig. 10. Results of Experiment 2 (2 cycle condition) reported as $1/(\text{motion direction threshold})$ versus temporal frequency. Symbols: LD 0.25 cyc/deg (o), LD 1.0 cyc/deg (\bullet), RG (x), YV (+). Top panel JSD, bottom, JES.

siderably greater for 16.7 and 25.0 Hz than it is for 1.0 Hz. Given the degrees of freedom available for psychophysical modeling (Graham, 1989), it would not be too difficult to build a model of the pedestal effect. To quantitatively model the motion-aftereffect, Sachtler and Zaidi (1993) found that they had to postulate directional motion units with some response to stationary stimuli. A similar property is evident in the motion-energy model of Adelson and Bergen (1985). The stationary pedestal will thus provide some impetus to direction selective units. It can be assumed that this impetus is much smaller for the unit detecting 16.7 Hz motion at threshold than for the slower unit detecting 1.0 Hz motion at threshold. In this case, it can be theorized in a manner similar to Nachmias and Sansbury (1974), that the pedestal moves the faster unit into the initial accelerating part of the contrast response function, whereas it moves the slower unit past the accelerating portion. However, this kind of modeling would not account for the 25.0 Hz data. At 25.0 Hz, without a pedestal, motion direction could not be dis-

criminated at any contrast, consistent with Morgan’s (1980) assumption that frequencies in the input higher than about 25.0 Hz are not represented as spatial movements at the level of the visual system where the visual directions of the targets are compared. The stationary pedestal has the remarkable effect of enabling the observer to discriminate motion-direction at 25.0 Hz.

When these experiments were performed (1994–1995), technological limitations precluded us from

MOTION DIRECTION ON ORTHOGONAL VS SAME COLOR PEDESTALS

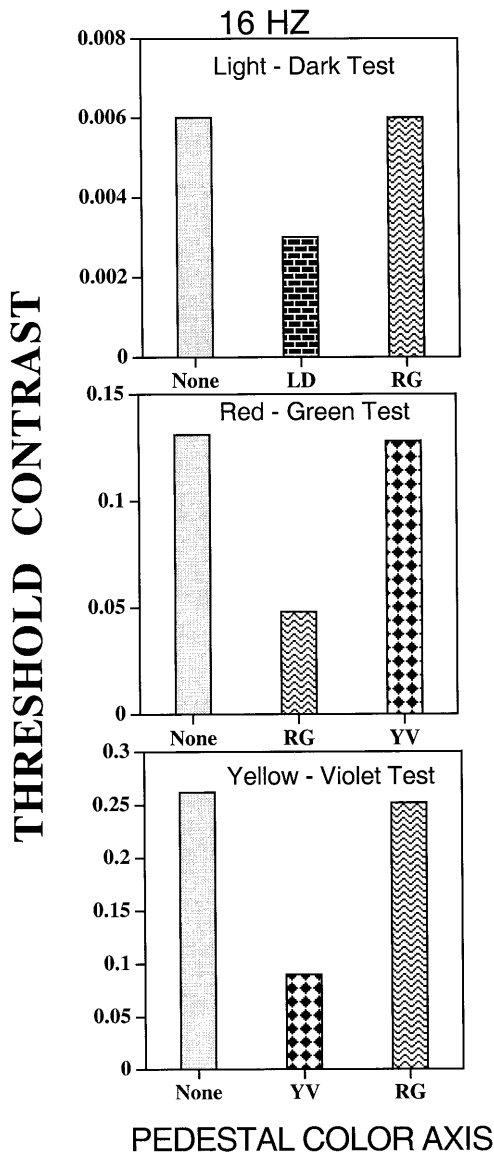


Fig. 11. Results of the first part of Experiment 3 (JSD). Threshold contrast for detecting motion direction is plotted against the pedestal conditions: No pedestal, pedestal along the same color axis as the moving grating, pedestal along an orthogonal color axis.

MOTION DIRECTION VS COUNTERPHASE MODULATION

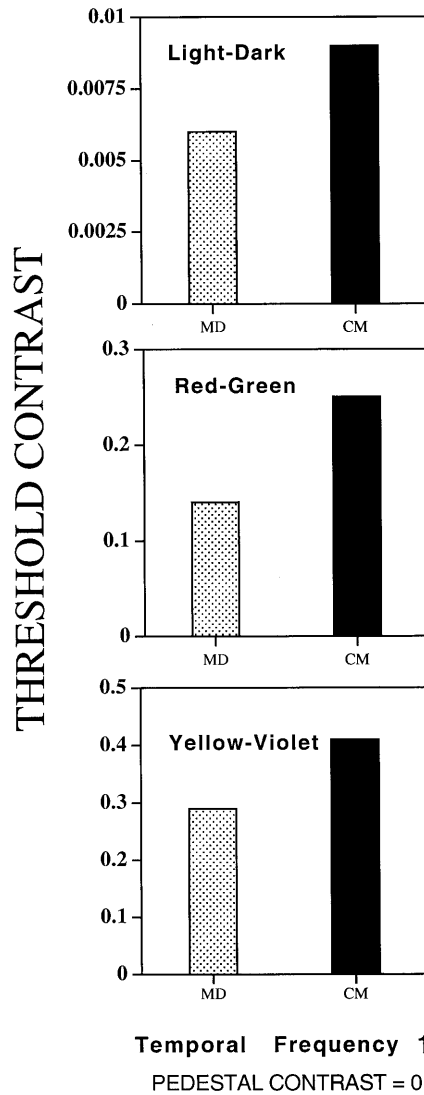


Fig. 12. Results of the second part of Experiment 3 (JSD). Threshold contrasts for detecting counterphase modulation and motion direction at 16 Hz are shown for each color axis.

showing smooth motion of less than 1.0 deg/s on top of stationary pedestals. A velocity of 1.0 deg/s is considered to be the minimum at which direction is judged correctly at threshold (Watson et al., 1980; Thompson, 1984; Mansfield & Nachmias, 1981). Now that it is possible for us to display slower velocities, we are using variants of the methods in this paper to study the separation between the domains of position-tracking and motion-energy, i.e. the minimum velocity required for motion-energy detection (Morikawa & Zaidi, 1999). Preliminary data suggest that there may be a significant age effect on the requisite minimum velocity; thus the techniques in this paper may have applications in detecting changes in the nervous system.

Acknowledgements

This work was supported by NEI grant EY07556. The results in this paper were presented at OSA 1994, ARVO 1995 and ECVF 1995. We thank Andrea Li, Kaz Morikawa, Jeanette Meng, Fuzz Griffiths and Byung-Geun Khang for extended discussions on this material, and Roshni Desai and Jodi Pukl for help with manuscript preparation.

References

- Adelson, E. H., & Bergen, J. R. (1985). Spatiotemporal energy models for the perception of motion. *Journal of the Optical Society of America, A*, 2, 284–299.
- Adelson, E. H., & Movshon, J. A. (1982). Phenomenal coherence of moving visual patterns. *Nature*, 300, 523–525.
- Albright, T. D. (1984). Direction and orientation selectivity of neurons in visual area MT of the macaque. *Journal of Neurophysiology*, 52, 1106–1130.
- Braddick, O. (1980). Low-level and high-level processes in apparent motion. *Philosophical Transactions of the Royal Society of London, B*, 290, 137–151.
- Bracewell, R. N. (1995). *Two dimensional imaging*. New Jersey: Prentice Hall.
- Cavanagh, P. (1992). Attention-based motion perception. *Science*, 257, 1563–1565.
- Cavanagh, P., Tyler, C. W., & Favreau, O. E. (1984). Perceived velocity of moving chromatic gratings. *Journal of the Optical Society of America, A1*, 893–899.
- Chubb, C., & Sperling, G. (1988). Drift-balanced random stimuli: a general basis for studying non-Fourier motion perception. *Journal of the Optical Society of America, A*, 5, 1986–2006.
- Chubb, C., & Sperling, G. (1989). Second-order motion perception: Space-time separable mechanisms. Proceedings: Workshop on Visual Motion, March 20–22, 1989 (pp. 126–138). Washington, DC: Computer Society Press of the IEEE.
- Cropper, S. J., & Derrington, A. M. (1996). Rapid colour-specific detection of motion in human vision. *Nature*, 379, 72–74.
- De Bonet, J. S., & Zaidi, Q. (1995). Temporal and spatial frequency analysis of motion-energy and feature-tracking. *Perception*, S24, 101.
- Derrington, A. M., Krauskopf, J., & Lennie, P. (1984). Chromatic mechanisms in lateral geniculate nucleus of macaque. *Journal of Physiology*, 357, 241–265.
- Emerson, R. C., Bergen, J. R., & Adelson, E. H. (1992). Directionally selective complex cells and the computation of motion energy in cat visual cortex. *Vision Research*, 32, 203–218.
- Exner, S. (1875). Experimentelle Untersuchung der einfachsten psychischen Prozesse. *Archiv für die Gesamte Physiologie des Menschen und der Tiere*, 11, 403–432.
- Gegenfurtner, K. R., & Hawken, M. J. (1996). Perceived velocity of luminance, chromatic and non-Fourier stimuli: influence of contrast and temporal frequency. *Vision Research*, 36, 1281–1290.
- Gegenfurtner, K. R., Kiper, D. C., & Levitt, J. B. (1997). Functional properties of neurons in macaque area V3. *Journal of Neurophysiology*, 77, 1906–1923.
- Gegenfurtner, K., Kiper, D., Beusmans, J., Carandini, M., Zaidi, Q., & Movshon, J. A. (1994). Chromatic properties of neurons in macaque MT. *Visual Neuroscience*, 11, 455–466.
- Graham, N. (1989). *Visual pattern analyzers*. New York: Oxford University Press.
- Gros, B. L., Pope, D. R., & Cohn, T. E. (1996). Relative efficiency for the detection of apparent motion. *Vision Research*, 36, 2297–2302.
- Hawken, M. J., Gegenfurtner, K. R., & Tang, C. (1994). Contrast dependence of colour and luminance motion mechanisms in human vision. *Nature*, 367, 268–270.
- Hochberg, J., & Brooks, V. (1978). The perception of motion pictures. In E. C. Carterette, & M. Friedman, *Handbook of perception*, vol. 10. New York: Academic Press.
- Hubel, D. H., & Wiesel, T. N. (1959). Receptive fields of single neurones in the cat's striate cortex. *Journal of Physiology (London)*, 148, 574–591.
- Johnston, A., & Clifford, C. W. G. (1995). Perceived motion of contrast-modulated gratings: predictions of the multi-channel gradient model and the role of full-wave rectification. *Vision Research*, 35, 1771–1783.
- Julesz, B. (1971). *Foundations of cyclopean perception*. Chicago, IL: University of Chicago Press.
- Kiper, D. C., Fenstemaker, S. B., & Gegenfurtner, K. R. (1997). Chromatic properties of neurons in macaque area V2. *Visual Neuroscience*, 14, 1061–1072.
- Krauskopf, J., & Farrell, B. (1991). Vernier acuity: effects of chromatic content, blur and contrast. *Vision Research*, 31, 735–749.
- Krauskopf, J., Williams, D. R., & Heeley, D. (1982). Cardinal directions of color space. *Vision Research*, 22, 1123–1131.
- Kulikowski, J., & Toulhurst, D. J. (1973). Psychophysical evidence for sustained and transient neurones in the human visual system. *Journal of Physiology*, 232, 149–162.
- Lennie, P. (1998). Single units and visual cortical organization. *Perception*, 27, 889–935.
- Lennie, P., Krauskopf, J., & Sclar, G. (1990). Chromatic mechanisms in striate cortex of macaque. *Journal of Neuroscience*, 10, 649–669.
- Lu, Z.-L., & Sperling, G. (1995). The functional architecture of human visual motion perception. *Vision Research*, 35, 2697–2722.
- Mansfield, R. J. W., & Nachmias, J. (1981). Perceived direction of motion under retinal image stabilization. *Vision Research*, 21, 1423–1425.
- Morgan, M. J. (1979). Perception of continuity in stroboscopic motion: a temporal frequency analysis. *Vision Research*, 19, 491–500.
- Morgan, M. J. (1980). Analogue models of motion perception. *Philosophical Transactions of the Royal Society of London, B*, 290, 117–135.
- Morikawa, K., & Zaidi, Q. (1999). Minimum velocity limits for motion energy detection. *Investigative Ophthalmology and Visual Science*, 40, S191.
- Nachmias, J., & Sansbury, R. V. (1974). Grating contrast: discrimination may be better than detection. *Vision Research*, 14, 1039–1042.
- Pearson, D. E. (1975). *Transmission and display of pictorial information*. New York: Wiley.
- Ramachandran, V. S., Rao, V. M., & Vidyasagar, T. R. (1973). Apparent movement with subjective contours. *Vision Research*, 13, 1399–1401.
- Reppas, J. B., Niyogi, S., Dale, A. M., Sereno, M. I., & Tootell, R. B. (1997). Representation of motion boundaries in retinotopic human visual cortical areas. *Nature*, 388, 175–179.
- Ronchi, V. (1957). *Optics: the science of vision*. NYU: NYU Press.
- Sachtler, W. L., & Zaidi, Q. (1993). Effect of spatial configuration on motion aftereffects. *Journal of the Optical Society of America, A*, 10, 1433–1449.
- Sachtler, W. L., & Zaidi, Q. (1995). Visual processing of motion boundaries. *Vision Research*, 35, 807–826.

- Stromeyer, C. F., Madsen, J. C., Klein, S., & Zeevi, Y. Y. (1978). Movement selective mechanisms in human vision sensitive to high spatial frequencies. *Journal of the Optical Society of America*, *68*, 1002–1005.
- Thompson, P. (1982). Perceived rate of movement depends on contrast. *Vision Research*, *22*, 377–380.
- Thompson, P. (1984). The coding of velocity of movement in the human visual system. *Vision Research*, *24*, 41–45.
- van Santen, J. P., & Sperling, G. (1985). Elaborated Reichardt detectors. *Journal of the Optical Society of America*, *A*, *2*(2), 300–321.
- Watson, A. B., & Ahumada, A. J. Jr. (1985). Model of human visual-motion sensing. *Journal of the Optical Society of America*, *A*, *2*(2), 322–341.
- Watson, A. B., Thompson, P. G., Murphy, B. J., & Nachmias, J. (1980). Summation and discrimination of gratings moving in opposite directions. *Vision Research*, *20*, 341–347.
- Wohlgemuth, A. (1911). On the aftereffect of seen movement. *British Journal of Psychology and Monography Supplement*, *1*, 1–117.
- Wuerger, S., Shapley, R., & Rubin, N. (1996). On the visually perceived direction of motion by Hans Wallach: 60 years later. *Perception*, *25*, 1317–1367.
- Yager, D., & Lapierre, N. (1975). Color and movement are processed separately: psychophysical evidence. *Modern Problems in Ophthalmology*, *17*, 357–363.
- Zaidi, Q., & Halevy, D. (1993). Visual mechanisms that signal the direction of color changes. *Vision Research*, *69*, 1037–1051.
- Zemany, L., Stromeyer, C. F. III, Chaparro, A., & Kronauer, R. E. (1998). Motion detection on flashed, stationary pedestal gratings: evidence for an opponent-motion mechanism. *Vision Research*, *38*(6), 795–812.